Infra-red measurements on one-way drawn poly(ethylene terephthalalate) films subjected to constant strain

I. J. Hutchinson* and I. M. Ward
Department of Physics, University of Leeds, Leeds LS2 9JT, UK
and H. A. Willis and Veronica Zichy
Research Department, ICI Ltd, Plastics Division, Welwyn Garden City, Herts, UK
(Received 21 February 1979)

The infra-red spectrum of one-way drawn PET film was measured as a function of further applied strain, the specimens being maintained under fixed strain, while the spectra were obtained for the two polarization situations where the electric vector is, respectively, parallel and perpendicular to the draw direction. The changes in molecular orientation and conformation were determined from the reconstruction procedures outlined as a function of applied strain. The spectra, together with those of poly(ethylene terephthalate) (PET) in several different structural forms were reconstructed over the frequency range 700–1100 cm^{-1} by a computational procedure using the method of damped least-squares. The minimum number of bands required to reconstruct all the spectra was chosen, and the existence of such bands in the second derivative spectrum was used as a criterion for their validity. With the exception of bands at 726 and 733 cm^{-1}, final fits were obtained on the basis that all the band shapes are Lorentzian. Comparison of the spectra of a number of model compounds showed that in nearly all cases the minor bands revealed by the curve fitting procedures could be identified with bands in the model compounds. It proved possible to relate the observed changes in the infra-red spectrum to the relaxed stress–strain curve of the film. The following picture emerges from the results for frequency shifts and changes in intensity. Up to the yield point there is considerable stress in the *trans* conformers (as reported by previous workers) and also in most of the *gauche* conformers. There is also a substantial increase in *trans* orientation, in contrast to the orientation of the terephthalate residue, which remains at the level observed at zero stress. The yield point marks the region where the stress on the *trans* and *gauche* conformers shows a sudden fall. At the same time there is a rapid increase in the *trans–gauche* ratio, a fall in the *trans* orientation, but an increase in the orientation of the terephthalate residues. It appears from these results that up to the yield point the elastic strains are concentrated in the glycol residues. After yield, both the stress and orientation decrease because conformational changes take place which allow the overall network structure to rearrange. When this occurs, there is some stress relaxation associated with the permanent flow, and the network as a whole achieves a higher degree of overall orientation, which is shown by changes in the orientation of the terephthalate residues. Subsequent deformation causes systematic changes in conformer content and molecular orientation which are consistent with continuum models for the plastic deformation of polymers.

INTRODUCTION

The present studies concern changes in molecular orientation and conformation which occur when an oriented polymer sample is extended. They relate directly to previous work where the changes in the infra-red spectrum of poly(ethylene terephthalate) (PET) due to permanent plastic deformation were reported[1]. These involve measurement of molecular orientation using bands characteristic of both the benzene ring and the glycol residue in either its *trans* or *gauche* conformation together with quantitative determination of the changes in concentration of these conformations as a function of the degree of plastic deformation. By monitoring these changes during the subsequent extension of a sample which has already been oriented, considerable insight can be gained into the molecular changes associated with the initial recoverable extension, the yield point and the subsequent strain-hardening behaviour.

Recently, studies have been carried out into changes in the infra-red spectra of polymers due to the application of stress[2–4]. In these investigations, a typical experiment is to subject an oriented polymer to tensile loading along the original draw direction and to determine the changes in position, intensity and band shape of certain 'stress-sensitive' bands. The interpretation of such experiments has been in terms of an inhomogeneous distribution of stress at a molecular level leading to certain molecular bonds being 'overstressed'. The relationship of such changes in the infra-red spectrum to mechanical behaviour has been suggested, both to fracture[2] and to stress relaxation and creep[4]. Using our method of spectrum reconstruction we have been able to define these frequency shifts more precisely on more absorption bands, and over a greater range of sample extension.

* Present address: ICI Corporate Laboratory, The Heath, Runcorn, Cheshire, UK

0032–3861/80/010055–11$02.00

EXPERIMENTAL

Materials

All measurements were carried out on a sample of one-way drawn PET film of thickness 0.03 mm. The sample had been prepared by drawing an amorphous melt-extruded sheet of PET at constant width between moving rollers at about 90°C. The ratio of the speeds of the feed roll to the drawn roll was set to give a nominal draw ratio of 3.5.

Infra-red measurements

The infra-red absorption spectra were obtained using a Perkin–Elmer 157 double beam spectrometer equipped with a rock-salt prism, external recorder (Servoscribe 1A) and a wire grid polarizer (Cambridge Consultants Limited type IGT 255) fitted in the common beam of the spectrometer. Absorption measurements were made at normal incidence using a slow scanning speed (50 cm^{-1} min^{-1}) with the film sample sandwiched between potassium bromide plates with a very thin film of Nujol between each surface. The Nujol is a sufficiently adequate match for the polymer refractive index to eliminate the interference fringes arising from reflection at the film surface, and has low absorption in the spectral range studied here. The wire grid polarizer is 99.7% efficient in transmitting radiation in one plane only, and spectra were recorded for the plane of polarization parallel and perpendicular to the initial draw direction, respectively.

The use of a prism rather than a grating spectrometer has the advantage that the inherent instrument polarization is only moderate and varies little with wavelength, whereas with a grating a much larger variation with wavelength is observed. This contributes to a more constant signal energy throughout the spectrum when a polarizer is used. The critical frequency values were subsequently checked on the Perkin–Elmer 580 ratio-recording high resolution grating spectrometer when this instrument became available.

To obtain the infra-red spectra of the film under stress the following procedure was adopted. A specimen of dimensions 4.5 cm x 1.5 cm (x 0.03 mm thickness) was held in a jig between a fixed clamp and a moveable clamp. Two screwed rods passed through the moveable clamp so that the latter can extend the sample in steps to a series of fixed imposed strains. At each level of strain, using a fresh sample each time, infra-red measurements were carried out when major stress–relaxation in the sample had ceased, as indicated by subsidiary mechanical tests described below. First, the thickness of the sample was determined from the spacing of near infra-red interference fringes. These measurements were undertaken in the range 8400–6400 cm^{-1} using a Grubb–Parsons Spectromajor double beam grating spectrometer. The sample, still held in the jig, was then transferred to the Perkin–Elmer spectrometer and the potassium bromide plates and Nujol films added, as described above, for the absorption measurements.

Mechanical measurements

Following the procedures adopted in previous publications[5] the relaxed stress–strain curve for the film was determined, because this is comparable with the response which is determined in the infra-red measurements. The relaxed stress–strain curve was constructed from a series of stress–relaxation curves obtained for a set of fixed strains. Dumbbell samples of gauge dimension 4.5 cm x 1.5 cm were extended to fixed strains in an Instron tensile testing machine at a crosshead speed of 2.5 cm/min. This rate was chosen to be very close to that employed in the infra-red measurements. As in the case of the infra-red measurements a fresh sample was taken for each level of strain.

For comparative purposes, load–elongation curves were also measured on similar samples at crosshead speeds of 2.5 and 10 cm/min.

Refractive index measurements

The three principal refractive indices of the film were measured using an Abbé refractometer, after the samples had been removed from the infra-red stretching device and allowed to relax in a stress-free condition for at least 30 min.

ANALYSIS OF INFRA-RED SPECTRA

Preliminary studies showed that by direct examination of the spectrum the only peak in which a shift could be identified with any certainty was that at 973 cm^{-1}. Any changes in the intensity or shape of the bands were so affected by overall changes in the apparent baselines as to make quantitative measurements of changes in orientation or conformation impracticable. These changes made it necessary to follow a systematic procedure for reconstructing the overall spectrum in terms of the individual bands, thus overcoming the problems of band overlap.

It is convenient to discuss the various steps involved in the analysis of the spectra in turn.

(1) The complete spectrum over the range 700–1100 cm^{-1} was reconstructed. This was necessary to enable quantitative estimates to be made of changes in the bands which are of primary concern. The infra-red spectra were recorded in transmission. The data points were read off manually and converted by computer to absorbance. Initially, the baseline was assumed to be linear but with an adjustable slope. As the computer fits were improved, it was found that this background gradient decreased. The final fit for the unstressed film indicated a zero gradient corresponding to 100% transmission.

(2) Initial reconstructions of the spectra were attempted assuming that the lineshapes (in terms of absorbance) could be intermediate between Gaussian and Lorentzian. Each band was represented by the superposition of two bands with identical peak positions, but with Gaussian and Lorentzian shape, respectively. It was found that in general there was no advantage to be gained by assuming other than a pure Lorentzian lineshape. The final fits were therefore obtained on the basis that all the band shapes are Lorentzian, with the exception of the bands at 726 and 733 cm^{-1} (to be discussed further below) where a mixture of 70% Lorentzian and 30% Gaussian was assumed. In the case of the very intense bands at ~1016 and ~875 cm^{-1} only those portions of the spectra at high transmittance were used, to eliminate instrumental distortion. For example, the 875 cm^{-1} band was fitted up to 20% transmission for the plane of polarization perpendicular to the draw direction and up to 10% transmission for the plane of polarization parallel to the draw direction.

(3) The final fit to the spectrum of the one-way drawn film showing the individual bands, is shown in *Figures 1* and *2*. It can be seen that there are many small bands which are not immediately apparent in the spectrum by mere inspection, but are clearly necessary to obtain a good fit. The identification of these bands was assisted by the examination of a number of samples of PET of different structure, in

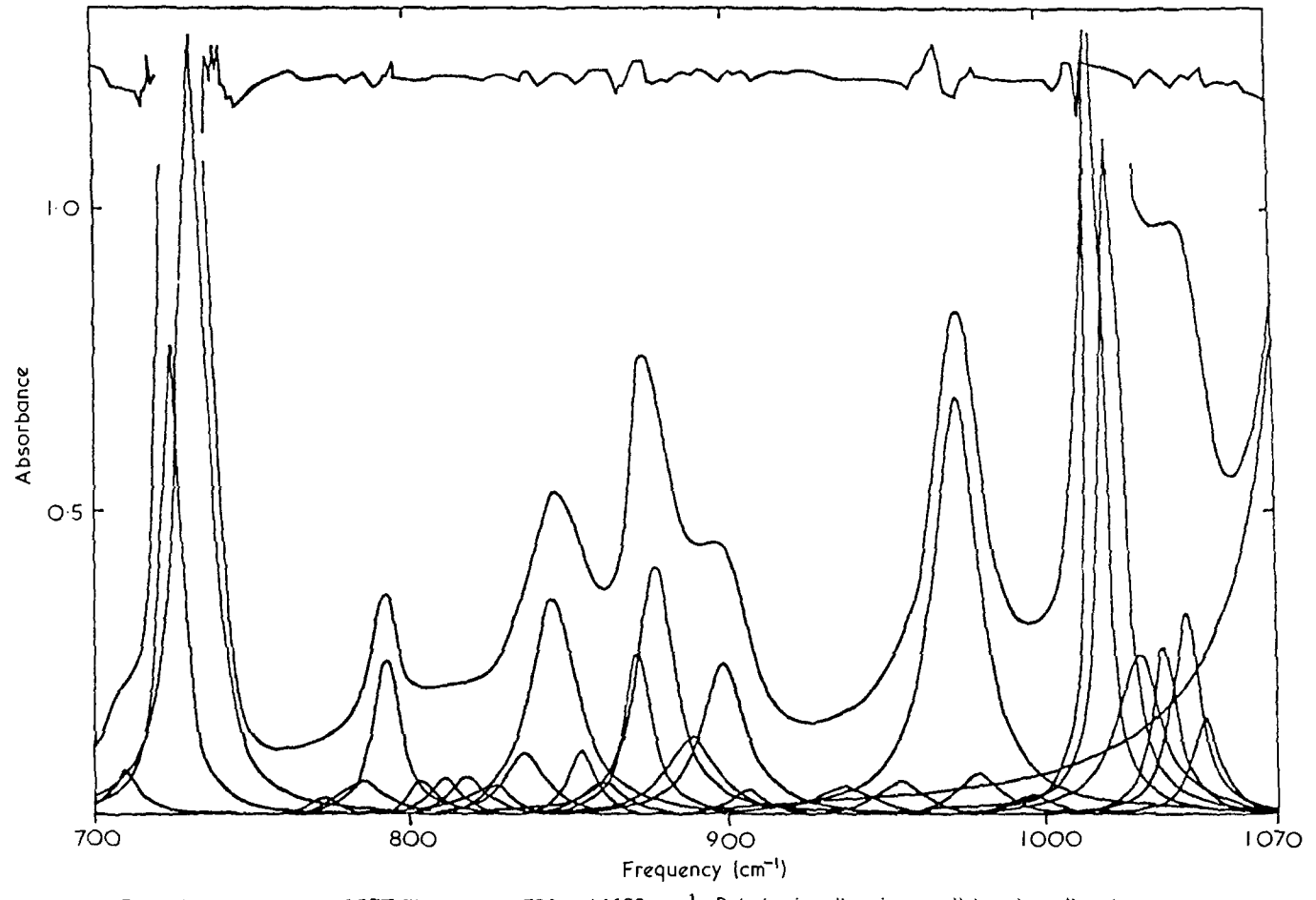

Figure 1 The infra-red spectrum of PET film between 700 and 1100 cm^{-1}. Polarization direction parallel to draw direction

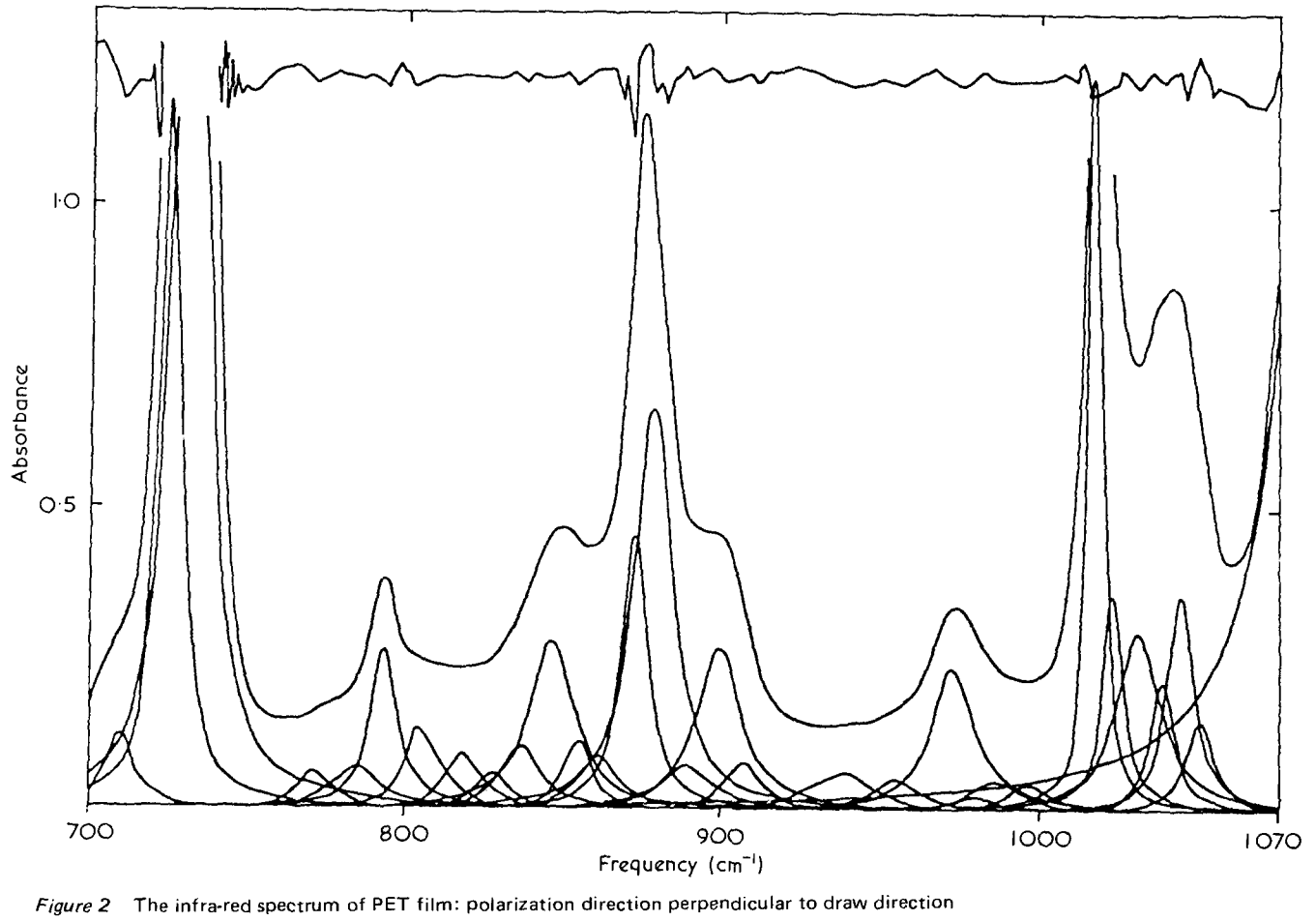

Figure 2 The infra-red spectrum of PET film: polarization direction perpendicular to draw direction

Table 1 Peak positions, half width and other details of absorption bands

Band frequency cm^{-1}	Half width cm^{-1}	Polarization	Intensity	Comments
709	11.4	σ	w	Present in LM
726*	8.2	σ	vs	Major band in PET
733*	10.8	σ	vs	Krimm assigns to $\delta(CH)_R$
733	10.0	—	vw	Present in C3B, C4 and C2A
785	17.4	σ	vw	Present in C3A Manley and Williams assign to $\delta(CH)_R$
793	9.7	—	m	Major band in PET
805	8.7	σ	vw	Present in C3B, EGB
811	10.6	—	vw	Present in C3A, C2A
819	11.2	—	vw	Present in C3B, LM
828	10.6	—	vw	No band in model compounds
837	14.6	—	w	Present in C3B, C4
846	17.0	π	m	Major band in PET
854	9.2	—	vw	Present in C3A, C4, C2A, C2B
861	14.1	σ	w	[Present in ethylene glycol]
873	9.5	σ	s	Major band in PET
878	13.8	σ	s	Major band in PET
889	18.8	π	w	Present in all cyclic oligomers
899	16.7	—	m	Major band in PET
907	12.4	—	vw	Present in EGB
937	21.1	—	vw	Present in C4, C2A, EGB
955	16.3	σ	vw	No band in model compounds
973	16.7	π	s	Major band in PET
979	14.9	σ	vw	Present in EGB and terephthalic acid
986	15.7	—	vw	Present in C5, C2A and L4
996	13.8	σ	vw	Present in C2A and terephthalic acid Manley and Williams assign to $\delta(CH)_R$
1017	4.7	π	vs	Major band in PET
1020	8.0	π	vs	Major band in PET
1031	17.7	—	m	Present in C3A, C3B
1039	9.3	π	m	Present in C4, C5, C2A
1045	10.0	—	m	Major band in PET
1051	9.7	—	m	Major band in PET
1086	10.6	π	vs	Major band in PET
1095	9.5	π	vs	Major band in PET. Present in most cyclic oligomers
1101	14.2	σ	vs	Major band in PET. Present in linear oligomers
1108	12.5	σ	vs	Major band in PET. Present in most cyclic oligomers
1122	18.0	π	vs	Major band in PET. Present in C5 and linear oligomers

addition to the one-way drawn film. These included: (a) one-way drawn film annealed at constant length; (b) one-way drawn film annealed without constraint; (c) amorphous film; (d) two-way drawn film; (e) one-way drawn film held at 20% strain.

In obtaining fits to these spectra, small changes in the band positions and half-widths were allowed. For oriented specimens where different polarization situations exist the band positions and half-widths were made identical for the two cases where the polarization directions are parallel to the draw direction and perpendicular to the draw direction in the plane of the film. The minimum number of bands necessary to reconstruct all the spectra was chosen, and the existence of such bands in the second derivative spectrum was used as a criterion for their validity. The second derivative spectra were obtained following the technique described by Savitsky and Golay[6]. To apply this method, data at fixed frequency intervals data are required. The peak intensities of the most intense absorption bands were therefore artificially reduced in magnitude at the computational stage and the second derivative data near such peaks ignored. Examination of histograms showing the number of times a peak appears in the second derivative spectra was used as a guide to the presence of weak bands.

The position, half-width and polarization of the bands obtained in the final fit are listed in *Table 1*. At this stage it was considered desirable to gain further confidence in the curve-fitting procedures by examining the spectra of model compounds. These included cyclic tris(ethylene terephthalate) in its crystallographic A and B forms (C3A and C3B), the cyclic tetra(ethylene terephthalate) (C5), the cyclic dimer ethylene terephthalate–diethylene terephthalate (C2A) and the cyclic dimer bis(diethylene terephthalate) (C2B). All these spectra were obtained with the kind assistance of Mr. G. Ogilvy, ICI Ltd, Fibres Division, Harrogate. Also examined was the spectra of the linear tetramer:

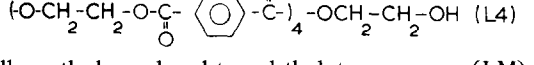

(L4)

as well as ethylene glycol terephthalate monomer (LM) and ethylene glycol dibenzoate (EGB) reported by Manley and Williams[7].

A careful examination of the spectra of all these compounds with the fitted spectrum for the one-way drawn film was then undertaken, taking into account the previous studies of many other workers, including Krimm[8,9], Miyake[10], Manley and Williams[7], Bahl, Cornell, Boerio and McGraw[11], and Ward and coworkers[12–15]. In nearly all cases the minor

bands revealed by the curve fitting procedures can be identified with bands in the spectra of the model compounds, and where this is so it is indicated in *Table 1*. There are only two bands, (at 828 and 955 cm^{-1}), for which there is no counterpart in the model compounds.

(4) To recapitulate, the curve fitting programme fits the set of Lorentzian shaped bands listed in *Table 1* to the measured absorbance spectrum using the method of damped least-squares due to Levenberg[16]. The spectra were fitted in pairs corresponding to the two measured polarization directions, maintaining the peak positions and half-widths constant within each pair.

The actual procedures for calculating the orientation functions and concentrations of absorbing species followed those described by Cunningham, Davies and Ward[17]. There are essentially two steps in the calculation. First, there is the reflectivity correction required to obtain the true absorbance k_i for a given polarization direction i from the measured optical density.

The argument presented in the previous publication gives the experimentally determined absorbance A_i as:

$$A_i = 0.4343\left(4\pi k_i \frac{y_0}{\lambda} + \frac{2k_i^2}{(n_i + n_{KBr})^2}\right) \quad (1)$$

where y_0 is the film thickness, λ the infra-red wavelength, and n_i and n_{KBr} the refractive index of the polymer and KBr, respectively. (We have corrected equation (12) of the previous publication where a factor of 2π was omitted from the first term. This makes the reflectivity correction even smaller, and in most circumstances it is negligible).

Following the previous work we now use this value of k_i to calculate the quantities $\phi_i = 4\pi N\langle\alpha_i''\rangle/3$ for intervals of 1 cm^{-1} where N is Avogadro's number and $\langle\alpha_i''\rangle$ the imaginary part of the molecular polarizability. In doing this, we affect the internal field correction, using equation (17) of the previous paper to obtain:

$$\phi_i = 6n_i k_i\{n_i^4 + 2n_i^2k_i^2 + 4n_i^2 - 4k_i^2 + k_i^4 + 4\}^{-1} \quad (2)$$

For small absorbance this can be approximated to:

$$\phi_i = \frac{6n_i k_i}{(n_i^2+2)^2}$$

It was considered most valid to use as a measure of the intensity of a given band the quantity:

$$\bar{\phi}_i = \int_{-\infty}^{\infty} \phi_i(\tilde{\lambda})d\tilde{\lambda}$$

For a Lorentzian lineshape assuming n is constant over the absorption line, this can be approximated to

$$\bar{\phi}_i = \frac{\pi}{2}\phi_i\Delta x_{1/2}$$

where $\Delta x_{1/2}$ is the half-bandwidth.

In the previous paper[17] it was shown that for a transversely isotropic film the concentration of absorbing species is proportional to

$$\bar{\phi}_0 = (\bar{\phi}_z + 2\bar{\phi}_x)/3$$

where $\bar{\phi}_z$, $\bar{\phi}_x$ describe the situations where the plane of polarization is parallel to the film draw direction and perpendicular to the film draw direction, in the plane of the film. For this one-way drawn film, the tilted film measurements show that $\bar{\phi}_y$, for the situation where the plane of polarization is perpendicular to the film draw direction and normal to the plane of the film is not equal to $\bar{\phi}_x$. The film has orthorhombic symmetry and in this case the concentration of absorbing species is proportional to:

$$\bar{\phi}_0 = \frac{1}{3}(\bar{\phi}_x + \bar{\phi}_y + \bar{\phi}_z) \quad (3)$$

In the previous paper it was also shown that for transverse isotropy the molecular orientation is given by:

$$\frac{\bar{\phi}_z - \bar{\phi}_x}{\bar{\phi}_z + 2\bar{\phi}_x} = P_2(\theta_m)\langle P_2(\theta)\rangle \quad (4)$$

where $P_2(\theta_m) = (3\cos^2\theta_m - 1)/2$ is a constant determined by the angle θ_m which a given transition dipole moment makes with the chain axis, and the orientation function $\langle P_2(\theta)\rangle$ describes the average value of $(3\cos^2\theta - 1)/2$ where θ is the angle made by a molecular chain-axis with the draw direction.

It has recently been shown, and has been discussed in detail in a separate publication[18], that for orthorhombic symmetry the relationship corresponding to equation (4) is:

$$\frac{2\bar{\phi}_z - \bar{\phi}_x - \bar{\phi}_y}{\bar{\phi}_z + 2\bar{\phi}_x} = 2P_{200}(\theta_m)\langle P_{200}(\theta)\rangle + 4\{1 - P_{200}(\theta_m)\}\langle P_{202}(\theta)\rangle \quad (5)$$

In this equation we have written P_{200} for P_2 and included a new spherical harmonic term $P_{202}(\theta)$ to take into account the reduction in symmetry from transverse isotropy to orthorhombic symmetry.

ANALYSIS OF REFRACTIVE INDEX MEASUREMENTS

Although ideally the principal refractive indices of the film should be measured under strain, in the absence of a practical method by which this could be achieved, the refractive indices were measured following each test, i.e. after the samples had been removed from the infra-red extensometer and allowed to relax. These values of refractive index were used in obtaining the infra-red susceptibility parameters $\bar{\phi}_i$. Bearing in mind that this internal field calculation is a comparatively minor correction to the direct estimate of orientation and conformer content from the infra-red absorbances, any errors introduced will be very small indeed.

The refractive index measurements are also of some interest in their own right as they provide additional measures of the molecular orientation. For a transversely isotropic film, it was shown in the previous paper[17] that:

$$\langle P_2(\theta)\rangle\frac{\Delta\alpha}{3\alpha_0} = \frac{\phi_z^e - \phi_x^e}{\phi_z^e + 2\phi_x^e} \quad (6)$$

Table 2 Values of $\bar{\phi}_x$, $\bar{\phi}_y$ and $\bar{\phi}_z$ for the one way drawn PET film, derived from the tilted film experiments

$\bar{\phi}_z$	$\bar{\phi}_x$	$\bar{\phi}_y$	Frequency (cm^{-1})
0.068	0.121	0.069	709
0.479	0.764	0.827	726*
1.035	1.720	3.216	733*
0.019	0.049	0.049	773
0.058	0.078	0.092	785
0.147	0.160	0.187	793
0.034	0.098	0.038	805
0.039	0.017	0.095	811
0.047	0.069	0.052	819
0.031	0.042	0.045	828
0.084	0.091	0.100	837
0.326	0.271	0.305	846
0.055	0.063	0.064	854
0.043	0.073	0.044	861
0.137	0.245	0.523	873
0.294	0.504	0.464	878
0.124	0.078	0.184	889
0.212	0.241	0.270	899
0.027	0.054	0.044	907
0.047	0.076	0.040	937
0.044	0.045	0.025	955
0.515	0.194	0.208	973
0.048	0.019	0.024	979
0.001	0.043	0.040	986
0.022	0.033	0.001	996
0.528	0.357	0.295	1017
0.527	0.180	0.302	1020
0.266	0.324	0.277	1031
0.152	0.120	0.143	1039
0.147	0.168	0.186	1045
0.070	0.068	0.106	1051

* Mixture of Lorentzian
\+ Gaussian line shapes

where $\langle P_2(\theta)\rangle$ refers to the overall molecular orientation and:

$$\phi_i^e = \frac{n_i^2 - 1}{n_i^2 + 2}$$

$\Delta\alpha/3\alpha_0$ can be estimated from the maximum birefringence of a highly oriented sample where $\langle P_2(\theta)\rangle = 1$.

The one-way drawn film possesses orthorhombic symmetry. It is shown elsewhere[18] that for this situation we have:

$$\frac{2\phi_z^e - \phi_x^e - \phi_y^e}{\phi_z^e + \phi_x^e + \phi_y^e} = \frac{2\Delta p}{3p_0}\langle P_{200}(\theta)\rangle + \frac{2\delta p}{p_0}\langle P_{202}(\theta)\rangle \qquad (7)$$

and

$$\frac{\phi_x^e - \phi_y^e}{\phi_z^e + \phi_x^e + \phi_y^e} = \frac{4\Delta p}{3p_0}\langle P_{220}(\theta)\rangle + \frac{2\delta p}{3p_0}\langle P_{222}(\theta)\rangle \qquad (8)$$

where p_1, p_2 and p_3 are the principal polarizabilities of a PET monomer and for convenience we define

$$\Delta p = p_1 - \frac{(p_2 + p_3)}{2}\ ;\ \delta p = p_3 - p_2$$

and

$$p_0 = \frac{1}{3}(p_1 + p_2 + p_3)$$

We have introduced three new spherical harmonic functions, the orientation functions $\langle P_{202}(\theta)\rangle$, $\langle P_{220}(\theta)\rangle$ and $\langle P_{222}(\theta)\rangle$ to describe the orientation of the film. We will only be concerned with equation (7) and $\langle P_{202}(\theta)\rangle$ and $\langle P_{200}(\theta)\rangle$ (which is equivalent to $\langle P_2(\theta)\rangle$ of equation 6). This provides an adequate link between the refractive index measurements and the infra-red measurements for the purposes of this paper. Following previous work, the values for the principal polarizabilities were taken as $p_1 = 1.22 \times 10^{-23}cm^3$; $p_2 = 2.12 \times 10^{-23}cm^3$; and $p_3 = 2.22 \times 10^{-23}cm^3$.

Characterization of the unstrained one-way drawn film

The unstrained one-way drawn film possesses orthorhombic symmetry. Its complete characterization is therefore much more complicated than for a film with transverse isotropy, and is the subject of another publication[18] which describes the results of infra-red and Raman spectroscopic measurements together with refractive index data. This very extensive study includes tilted film infra-red measurements which enable the out-of-plane quantities $\bar{\phi}_y$ to be calculated in addition to $\bar{\phi}_z$ and $\bar{\phi}_x$ which can be found from the straightforward measurements which have been undertaken in the strained samples. Without values of $\bar{\phi}_y$ for the strained samples, assumptions and approximations have been made so that the data can be examined on a quantitative basis. In this paper we will therefore take as our starting point the results for the unstrained film, leaving the detailed discussion of how they were obtained and their full significance for the separate publication[18].

Table 2 shows the values of $\bar{\phi}_x$, $\bar{\phi}_y$ and $\bar{\phi}_z$ for all the infra-red bands.

Although for many of the key bands the major anisotropy is between $\bar{\phi}_z$ and $\bar{\phi}_x$ or ϕ_y, which are approximately equal, this is not true in all cases, confirming that we have to take this into account. The refractive index results are shown in *Table 3*, and again although $n_x \neq n_y$, the major anisotropy is between n_z and n_x or n_y.

RESULTS AND DISCUSSION

Mechanical measurements

Figure 3 shows the stress-relaxation curves at different initial strains. It can be seen that up to the yield point at about 4% elongation, there is very little stress-relaxation. The relaxed stress–strain curve constructed from these stress–relaxation measurements is shown in *Figure 4*. It is interesting to note that this shows a clear yield drop followed by a region in which there is a gradual rise in nominal stress, the 'strain-hardening' region. For comparison, the load–elongation curves are shown in *Figure 5*. The yield point is

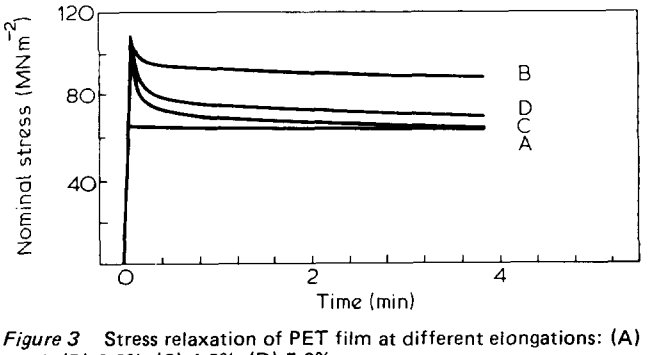

Figure 3 Stress relaxation of PET film at different elongations: (A) 1.3%; (B) 2.6%; (C) 4.0%; (D) 5.0%

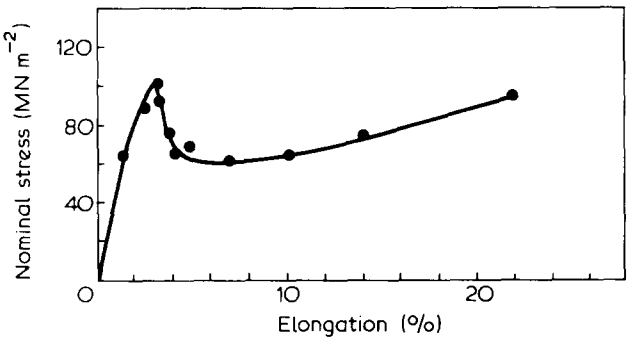

Figure 4 Relaxed stress–strain curve for PET

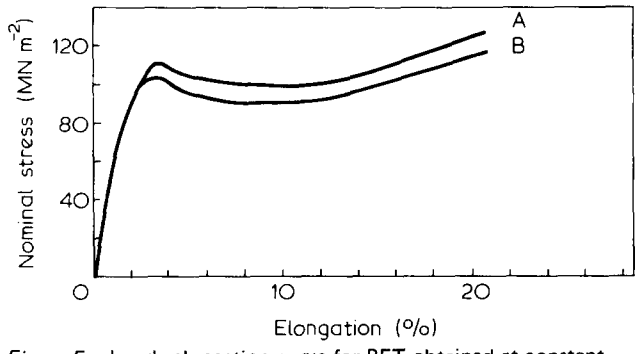

Figure 5 Load–elongation curve for PET obtained at constant crosshead speed: A, 10 cm min^{-1}; B, 2.5 cm min^{-1}

Table 3 Refractive index measurements

n_x = 1.543	n_y = 1.568	n_z = 1.637

again observed at about 4% elongation and there is some strain rate dependence, as would be expected.

These results are important because they highlight the fact that the yield point does seem to be related to the comparatively sudden onset of viscoelastic relaxation processes, and that up to this point the behaviour is elastic to a good first approximation. This is particularly important for the present investigation, because it encourages the possibility that the infra-red studies of the relaxed polymer under stress may be able to identify specific molecular changes associated with both yield and post yield processes and that the observation of a maximum in the stress–strain curve is not merely an indication of increasing strain rate with increasing stress.

Infra-red measurements

The band assignments for PET can be made on the basis of an isolated chain molecule[12–15]. It can be further assumed that the vibrational modes for the chain can be separated into those associated with the *para*-disubstituted benzene ring and those assocated with the glycol residue. It can be concluded from assessment of infra-red and Raman spectroscopic studies as well as other related work, that conformational changes occur involving both the glycol residue and the terephthalate residue[15]. To reduce the complexity of the discussion, there is some merit in considering the changes in bands associated with the benzene ring and glycol residue separately[15].

Benzene ring mode vibrations

The first band to be considered is that assigned to the ring B_{2u} C–H in plane bending vibration[15] which appears as a very strong doublet with components at 1017 and 1020 cm^{-1}, both of which show parallel dichroism. *Table 4* shows the relative integrated intensities of the two components for a range of PET samples. Although there is no simple identifiable connection between the relative intensities and the polymer morphology, it can be seen that the 1017 cm^{-1} component certainly decreases with increasing crystallinity and there is a corresponding increase in the 1020 cm^{-1} component. Therefore it can be tentatively concluded that the 1020 cm^{-1} component is associated with an ordered environment of chain molecules whereas the 1017 cm^{-1} component is associated with a disordered environment.

Figure 6 shows the concentration of the two species, plotted in terms of $\bar{\phi}_0$, as a function of applied strain. It can be seen that the 1020 cm^{-1} component shows a marked decrease in intensity up to 4% strain, with a corresponding increase in the intensity of the 1017 cm^{-1} component. This suggests that there is a loss of intermolecular order in the initial straining prior to yield. Beyond 4% there is a reversal of this behaviour and in the region of the yield drop, the 1020 cm^{-1} component decreases. These changes could be due to recrystallization following yield during the strain-hardening region.

If it is assumed that the extinction coefficients of these two components are identical, we can proceed to calculate the change in orientation with strain. We make two further assumptions. First, because the 1017/1020 cm^{-1} doublet is a parallel band where the transition moment vector makes the comparatively small angle ~20° with the chain axis, the term $4\{1 - P_{200}(\theta_m)\}\langle P_{202}(\theta)\rangle$ will be small compared with $2P_{200}(\theta_m)\langle P_{200}(\theta)\rangle$ in equation (5). Secondly the tilted film results for the unstrained film suggest that for

Table 4 Integrated intensity $3\bar{\phi}_0$ of the 1018 cm^{-1} band for different PET films

Material	1017 cm^{-1} component	1020 cm^{-1} component	Total
One way drawn film	1.180	1.009	2.189
One way drawn film heat set at 130°C for 10 min (no restraint)	0.545	0.979	1.524
One way drawn film heat set at 130°C for 10 min (restrained)	0.525	0.014	1.539
One way drawn film heat set at 220°C for 10 min (restrained)	0.546	1.078	1.624
Amorphous isotropic	0.442	0.975	1.418
Amorphous isotropic heat set at 150°C for 1 min (restrained)	0.326	1.848	2.174
Amorphous isotropic heat set at 150°C for 5 min (restrained)	0.337	1.598	1.935

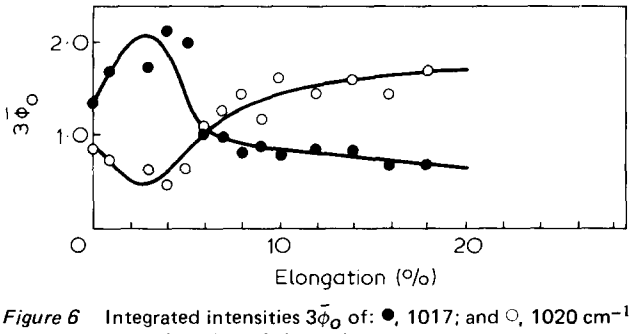

Figure 6 Integrated intensities $3\bar{\phi}_0$ of: ●, 1017; and ○, 1020 cm^{-1} components as a function of elongation

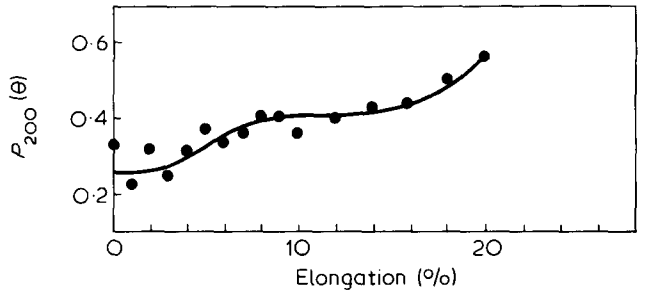

Figure 7 $P_{200}(\theta)$ for 1017/1020 cm^{-1} doublet as a function of elongation

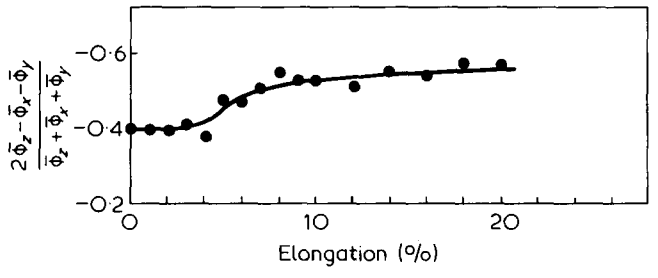

Figure 8 Orientation function $2\bar{\phi}_z - \bar{\phi}_x - \bar{\phi}_y/\bar{\phi}_z + \bar{\phi}_x + \bar{\phi}_y$ for 873/878 cm^{-1} doublet as a function of elongation

this doublet $\bar{\phi}_x = \bar{\phi}_y$ to a reasonable approximation. We can therefore write:

$$\frac{\bar{\phi}_z - \bar{\phi}_x}{\bar{\phi}_z + 2\bar{\phi}_x} = P_{200}(\theta_m)\langle P_{200}(\theta)\rangle \qquad (5a)$$

The calculated values of $\langle P_{200}(\theta)\rangle$ at each strain level are shown in *Figure 7*. There is considerable scatter in the results, which can be attributed to the high absorbance mentioned above, and the results for this doublet are very much less accurate than for all the other bands to be discussed. All that can be concluded is that the value of $P_{200}(\theta)$ remains constant within the experimental scatter at low strain, but that there is an overall increase in $P_{200}(\theta)$ over the whole range of elongation considered.

The next band to be considered is that at 875 cm^{-1} which has been assigned to a ring –CH out of plane deformation, possibly with a C–O–C bending deformation component[15]. It shows strong perpendicular dichroism and has been deconvoluted into two components with peaks at 873 and 878 cm^{-1}, respectively. The tilted film results on the unstrained film show that for this band $\bar{\phi}_y$ is greater than $\bar{\phi}_x$ or $\bar{\phi}_z$. As only $\bar{\phi}_z$ and $\bar{\phi}_x$ can be estimated for the strained samples, it is assumed that $\bar{\phi}_y/\bar{\phi}_x$ remains at the same value of 1.32 which was determined for the unstrained sample. With this assumption it is possible to develop the results in two ways. First, because θ_m is very close to 90° (the molecular model proposed in previous work suggests $\theta_m = 83°$) the term 4 $[1 - P_{200}(\theta_m)]$ $\langle P_{202}(\theta)\rangle$ in equation (5) is now significantly large. By assuming the values of $\langle P_{200}(\theta)\rangle$ calculated from the results for the 1017/1020 cm^{-1} doublet, values of $\langle P_{202}(\theta)\rangle$ can be obtained for the strained samples. These results indicate that $\langle P_{202}(\theta)\rangle$ does not change significantly with strain. Secondly, the values of the orientation function $2\bar{\phi}_z - \bar{\phi}_x - \bar{\phi}_y/\bar{\phi}_z + \bar{\phi}_x + \bar{\phi}_y$ can be calculated for the individual components and for the total doublet.

Figure 8 shows the overall orientation function for both components added together, as a function of applied strain. The results are qualitatively very similar to those obtained for the 1017/1020 cm^{-1} doublet but the measurements are much more precise and we can see that there is no significant change up to 4% strain; thereafter a rather rapid increase in orientation in the yield drop region followed by a more gradual increase in orientation up to the highest strain levels is recorded. When the changes in the two components are examined separately, it is found that the sudden change at 4% strain is due to changes in the orientation of the 873 cm^{-1} component (*Figure 9*). The 878 cm^{-1} component shows very little change (possibly a very slight decrease) up to 6% strain after which there is an increase in orientation. A possibility is that the 873 cm^{-1} band is associated with ordered regions and the 878 cm^{-1} band with disordered regions.

The other benzene ring band considered in this exercise was that at 735 cm^{-1}. This band shows strong perpendicular dichroism and has been deconvoluted into two components with peaks at 726 and 733 cm^{-1}. It was assumed that the extinction coefficients for the two components are equal and that the data can be treated in a similar manner to the 873/878 cm^{-1} doublet. *Figure 10* shows the change in $2\bar{\phi}_z - \bar{\phi}_x - \bar{\phi}_y/\bar{\phi}_z + \bar{\phi}_y + \bar{\phi}_z$ as a function of applied strain. Again, there is a very clear indication that there is no significant change up to 4% strain, followed by a rather rapid increase in the region 4–6%, with a more gradual increase subsequently.

In fitting these results for different strain levels the peak positions of the 1017, 1020, 873 and 878 cm^{-1} bands were allowed to vary. It was found, however, that the spread in frequency was small. This is shown in *Table 5*; it can be concluded that no systematic shift in frequency due to applied strain can be observed for these bands.

Glycol residue vibration mode absorptions

Following previous studies by ourselves and other workers[12–15,19–21] it is of particular interest to examine glycol residue bands which have been assigned to vibrations

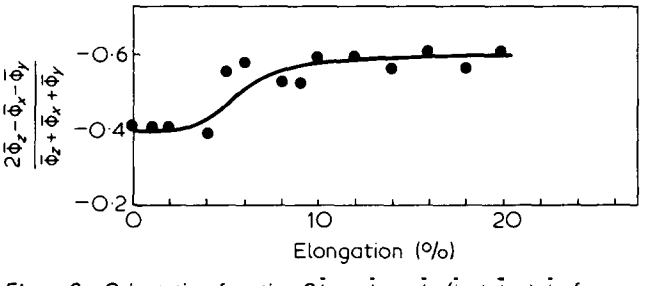

Figure 9 Orientation function $2\bar{\phi}_z - \bar{\phi}_x - \bar{\phi}_y/\bar{\phi}_z + \bar{\phi}_x + \bar{\phi}_y$ for 873 cm^{-1} component as a function of elongation

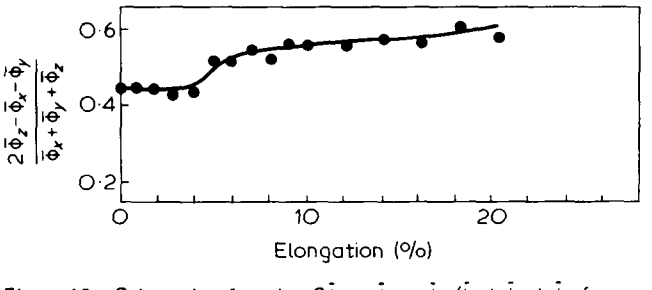

Figure 10 Orientation function $2\bar{\phi}_z - \bar{\phi}_x - \bar{\phi}_y/\bar{\phi}_z + \bar{\phi}_x + \bar{\phi}_y$ for 735 cm^{-1} band as a function of elongation

Table 5 Variation in frequency of benzene ring bands

Mean frequency cm^{-1}	Standard deviation cm^{-1}
1016.5	±0.6
1020.4	±0.7
872.9	±0.4
877.7	±0.7

of the *trans* and *gauche* conformations, respectively. Foremost amongst these are the two groups of bands centred on peaks at 973 and 899 cm^{-1}.

The group centred on the major *trans* band at 973 cm^{-1} includes a weak band at 979 cm^{-1}, and very weak bands at 986, 955 and 996 cm^{-1}. There is also another very weak band at 937 cm^{-1}. Of these bands only that at 973 cm^{-1} has been firmly assigned by many workers to a vibration of the *trans* conformation. It does seem likely, however, that these other weak bands could also be associated with *trans* conformations in different intermolecular environments. In particular the 979 cm^{-1} band virtually disappears in highly crystallized samples, and may therefore be ascribed to *trans* conformers in disordered regions.

The group centred on the major *gauche* band at 899 cm^{-1} includes a weak band at 889 cm^{-1} and a very weak band at 907 cm^{-1}. Again it is reasonable to propose that these bands can be associated with *gauche* conformation in different environments. The most favoured assignment has been to a CH_2 rocking mode (A_u).

Several workers have reported[2,4] that on subjecting highly drawn PET samples to stress, the frequency of the 973 cm^{-1} band decreases, and that there is a distortion of the low frequency wing of the band. Similar effects can be clearly seen in the original spectra of our strained samples. When the bands in the deconvoluted spectra are examined, however, it appears that of those at present under discussion, only the *trans* bands at 973 and 979 cm^{-1} and the *gauche* bands at 899, 907 and 889 cm^{-1} show a shift in frequency. The remaining bands at 937, 955, 986 and 996 cm^{-1} are all of such low intensity that they will have a negligible influence on consideration of the overall changes in orientation and conformation of the glycol residue. For this reason we will confine our discussion to consideration of the other more intense bands.

In dealing with the glycol residue bands we have simplified the analysis on the basis of the following considerations. Those bands assigned to *gauche* conformations show comparatively small dichroism and to a very good approximation $\bar{\phi}_x = \bar{\phi}_y$. Those bands associated with the *trans* conformation show strong parallel dichroism and again to a good approximation $\bar{\phi}_x = \bar{\phi}_y$. It is therefore reasonable to assume that for the purposes of examining the changes in both *gauche* and *trans* bands due to straining, the one-way drawn film is transversely isotropic. First, we will consider the band at 889 cm^{-1} which at first sight could be associated with the 899 cm^{-1} *gauche* band. It has already been noted that the frequency of this band changes under stress. However, it was found that there was no systematic change in the intensity, $\bar{\phi}_0$, of this band, which we will see is contrary to the behaviour of the 899 and 907 cm^{-1} bands. Furthermore there were no changes in orientation observed until after 4% strain, which is similar to the behaviour of the benzene ring mode bands. For this reason, we will leave the 899 cm^{-1} band out of our initial discussion and now discuss the changes in intensity of the 899/907 cm^{-1} *gauche* bands and the 973/979 cm^{-1} *trans* bands.

In our previous paper, we considered changes in the peak intensities of the apparent bands at 973 and 899 cm^{-1}. Excellent consistency was obtained by taking these as a measure of *trans* and *gauche* content respectively, on the basis that the extinction coefficients for the two bands were identical. We have therefore proceeded on the initial assumption that the extinction coefficients of all these four bands at 973, 979, 899 and 907 cm^{-1} are equal. In the present work, as already explained, the concentration of any absorbing species is related to integrated absorption and not to peak. It was found that the total integrated intensity for all four bands remained constant to a reasonable approximation. The results are summarized in *Figures 11* and *12*. *Figure 11* shows that up to 4% strain there is no significant change in *trans/gauche* content, but in the region 4–8% the *trans/gauche* ratio increases markedly, continuing to increase but at a slower rate with further increasing strain. It can be seen that the increase in *trans* content is exactly mirrored by the decrease in *gauche* content, confirming that the assumption of identical extinction coefficients is valid to a reasonable approximation. A further analysis of the two *trans* bands shows (*Figure 12*) that in the initial stages of elongation (up to 4%) there is a marked decrease in the intensity of the 973 cm^{-1} band accompanied by an increase in that of the 979 cm^{-1} band. This may be due to a loss of intermolecular order prior to yield as already shown by the behaviour of the 1020–1017 cm^{-1} pair of benzene ring modes. At higher strains, the intensity of both 973 and 979 cm^{-1} bands increases, reflecting the increase in total *trans* content.

Many previous workers[2,4] have reported that the 973 cm^{-1} band moves to lower frequency on application of applied load. Whereas the previous work has always been restricted to the initial portion of the stress–strain curve, we have now examined the spectra over a much greater region of strain. The results which we have obtained confirm that the shift to lower frequencies is clearly proportional to the applied load up to the yield point. Beyond the yield point more complex changes occur, and although the 973 cm^{-1} band remains constant at a frequency of approximately 970 cm^{-1}, the behaviour of the 979 cm^{-1} component appears to be more complicated. We have not had the opportunity to explore this fully, and recognize that it may be related to the complex changes in *trans* and *gauche* isomerism at the yield point referred to above.

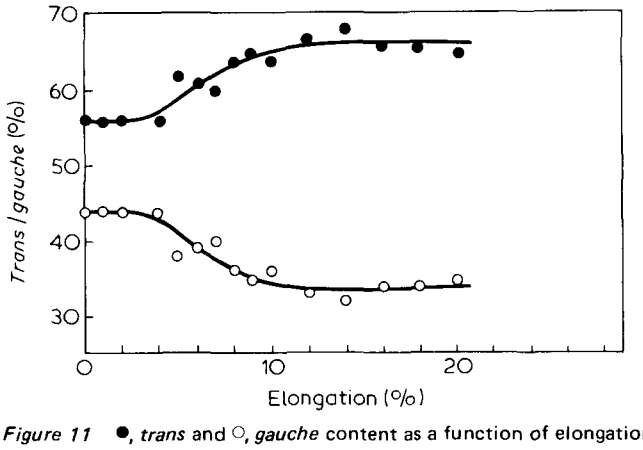

Figure 11 ●, *trans* and ○, *gauche* content as a function of elongation

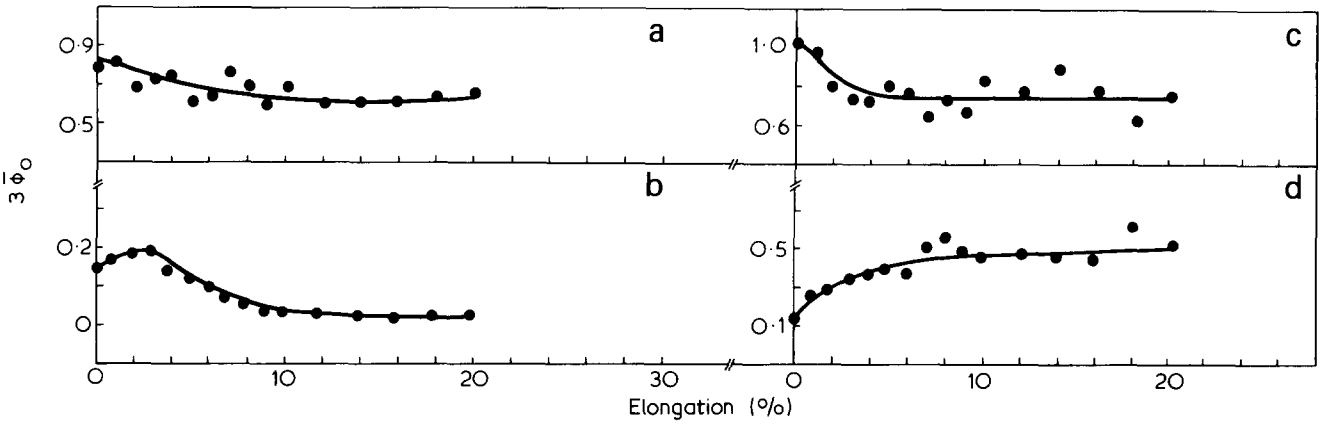

Figure 12 Integrated intensities $3\phi_\sigma$ bands assigned to *gauche* and *trans* conformers as a function of elongation: (a) 899 cm^{-1} *gauche*; (b) 907 cm^{-1} *gauche*; (c) 973 cm^{-1} *trans* (d) 979 cm^{-1} *trans*

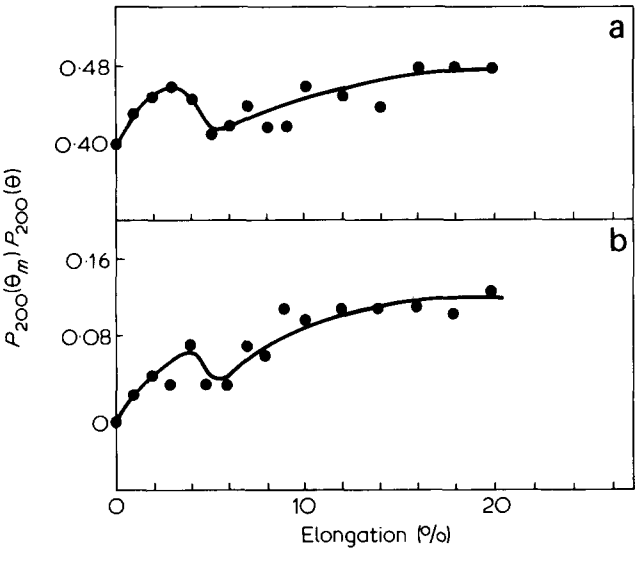

Figure 13 Orientation function $P_{200}(\theta_m)$ $P_{200}(\theta)$ as a function of elongation for: (a) 973/979 cm^{-1} *trans* doublet; and (b) 889/907 cm^{-1} *gauche* doublet

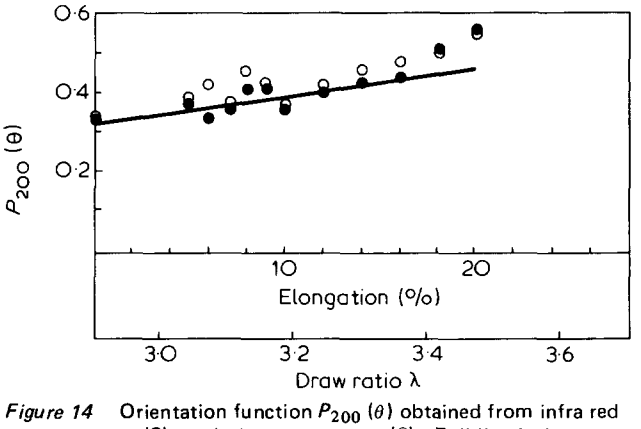

Figure 14 Orientation function $P_{200}(\theta)$ obtained from infra red measurements (●), optical measurements (○). Full line is that predicted by the rubber network model

The orientation functions also present quite a complex picture (*Figure 13*). It should be borne in mind that the 899 and 973 cm^{-1} bands are by far the most intense and that the results for these bands are therefore more accurate than for the other weaker bands. It appears that the orientation of both these bands follows a similar pattern. In contrast to the benzene ring mode bands there is a continuous increase in orientation from zero to 4% strain followed by a sudden decrease from 4% to 6% strain after which the orientation increases again. The 907 cm^{-1} band shows a gradual increase in orientation up to the 6–8% region where there is a sudden increase. The 979 cm^{-1} band shows a sudden increase in orientation in the low strain region of ~1% strain, after which there is little change.

The overall concentration figures $\bar{\phi}_0$ for these four bands reveal a similar complexity as a function of applied strain (*Figure 12*). It is very striking that the intensity of the 973 cm^{-1} band decreases up to 4% strain, whereas that of the 979 cm^{-1} increases, reflecting an approximately constant total *trans* content. After 4% strain, the intensities of both components increases and the *trans/gauche* ratio increases as shown previously.

A similar change occurs in the relative intensities of the *gauche* bands at 899 and 907 cm^{-1} prior to 4% strain, after which the overall intensities of both bands decrease.

The following picture emerges from these results for frequency shifts and changes in concentration and orientation. Up to the yield point, there is considerable stress on the *trans* conformers, shown by the frequency shifts in the 973 and 979 cm^{-1} bands, and also on most of the *gauche* conformers, those which give rise to the 899 cm^{-1} band. There is also a considerable increase in *trans* orientation in this low strain region, in contrast to the benzene ring orientation which remains at the unstrained level. In the region immediately beyond the 4% strain, the stress on these conformers is largely released and at the same time there is a sudden onset of an increase in the *trans/gauche* ratio and also a fall in the *trans* orientation

Comparison of infra-red and optical measurements and possible relevance of molecular network

In the previous publication[4] it was shown that for the plastic deformation of uniaxially-oriented PET, there was a good correlation between the orientation functions derived from infra-red and optical measurements. Moreover, it was shown that the changes in molecular orientations and conformer content were consistent with the stretching of a rubber like network.

The values of $\langle P_{200}(\theta)\rangle$ obtained from the 875 cm^{-1} band can also be combined with the refractive index measurement on the relaxed polymer to obtain an independent determination of $\langle P_{200}(\theta)\rangle$, using equation (7). The results are shown in *Figure 14*, from which it can be seen

that there is good agreement between the values of $\langle P_{200}(\theta)\rangle$ calculated from the infra-red and optical measurements. Also shown in the figure is a theoretical curve derived for the deformation of a rubber-like network of equivalent random links. This assumes that $\langle P_{200}(\theta)\rangle$ is given by[18]

$$\langle P_{200}(\theta)\rangle = \frac{1}{10N}(2\lambda_z^2 - \lambda_x^2 - \lambda_y^2) \quad (9)$$

where λ_x, λ_y, λ_z are the total extension ratios, i.e. including both the initial drawing and the subsequent straining in these experiments. N is the number of random links per chain and, following previous work[4], is taken to have the value 4.8. Although the nominal draw ratio is 3.5:1, the value of $\langle P_{200}(\theta)\rangle$ for the unstrained film suggests that the effective draw ratio is 2.9. It was assumed that deformation takes place at constant width so that $\lambda_x = 1$, $\lambda_z = \lambda = 1/\lambda_y$ throughout the deformation. *Figure 14* shows that there is reasonable agreement between the experimental results and the theoretical curve, suggesting that the plastic deformation processes which occur on straining the drawn film are similar to those which occur in the initial drawing process, and involve the stretching of a molecular network. Following the discussion of previous work[18] again, further confirmation for this is obtained from the change in conformer concentration with strain. In the previous paper,it was shown that the increase in *trans* conformer content with strain followed the form proposed by Abe and Flory[22]. For the orthorhombic symmetry sheet, the increase in *trans* concentration should be proportional to $\{1/3(\lambda^2 + 1 + 1/\lambda^2) - 1\}$. Our results are consistent with this linear relationship up to 14% strain, after which the *trans/gauche* conformational changes are exhausted.

CONCLUSIONS

The results obtained from refractive index measurements and from the benzene ring band orientation functions show that the orientation induced by permanent plastic deformation in PET i.e. occurring beyond the yield point, is consistent with the further orientation of the molecular network. The results for the glycol residue bands show that, up to the yield point, the elastic strains are concentrated in the glycol residue, leading to the frequency shifts in the bands associated with *trans* and *gauche* conformers and to orientation of these parts of the chain. After yield both the stress and the orientation decrease, because the conformational changes can take place to allow the overall network structure to rearrange. When this occurs, stress relaxation associated with permanent plastic flow takes place and the network as a whole achieves a higher state of overall orientation, reflected by the changes in benzene ring orientation and birefringence. Although there is some viscoelasticity before the yield point, it is clear that this marks a unique point. It could be that the stresses localized in the glycol residue lead to the burst of *gauche* conformers defined in the Robertson theory of yield[23]. This rapid process would not be seen in these measurements. Perhaps the clearest points which emerge from the present measurements are (1) the constant benzene ring orientation up to 4% strain followed by a gradual increase consistent with the rubber network deformation scheme, (2) the constant *trans/gauche* ratio up to 4% strain followed by a gradual increase in this ratio, as required by the rubber network deformation scheme.

It will be noted that the reconstruction procedures which have been adopted in this study remove entirely the necessity to postulate that there are changes in band shape, as well as intensity and peak positions when PET film are under stress. We have shown that although our results confirm the shifts in peak position of the 975 cm^{-1} band reported by previous workers, the changes in shape can be attributed entirely to changes in the orientation of the *trans* species giving rise to the minor bands at 937 and 955 cm^{-1}. It is important to note that there are no changes in the overall concentration of these species as determined from $\bar{\phi}_0$ for these bands.

ACKNOWLEDGEMENTS

We are indebted to Imperial Chemical Industries, Plastics Division as the industrial sponsor of the SRC CASE studentship which supported I. J. Hutchinson during this research.

REFERENCES

1 Cunningham, A., Ward, I. M., Willis, H. A. and Zichy, V. I. *Polymer* 1974, **15**, 749
2 Zhurkov, S. N., Vettegren, V. I., Korsukov, V. E. and Novak, I. I. 'Fracture' in 'Proceedings of the Second International Conference on Fracture, Brighton, England', Chapman and Hall, London, 1969, p 545
3 Roylance, D. K. and de Vries, K. L. *Polym. Lett.* 1971, **9**, 443
4 Wool, R. P. and Statton, W. O. *J. Polym. Sci.* 1974, **12**, 1575
5 Brereton, M. G., Davies, G. R., Jakeways, R., Smith, T. and Ward, I. M. *Polymer* 1978, **19**, 17
6 Savitsky, A. and Golay, M. J. E. *Anal-Chem.* 1964, **36**, 1627
7 Manley, T. R. and Williams, D. A. *Polymer* 1969, **10**, 339
8 Liang, C. Y. and Krimm, S. *J. Mol Spectrosc.* 1959, **3**, 554
9 Krimm, S. *Adv. Polym. Sci.* 1960, **2**, 51
10 Mijake, A. *J. Polym. Sci.* 1959, **38**, 497
11 Bahl, S. K., Cornell, D. D., Boerio, F. J. and McGraw, G. E. *J. Polym. Sci., Polym. Lett.* 1974, **12**, 13
12 Grime, D. and Ward, I. M. *Trans. Faraday Soc.* 1958, **54**, 959
13 Ward, I. M. *Chem. Ind. (London)* 1956, p 905
14 Farrow, G., McIntosh, J. and Ward, I. M. *Makromol. Chem.* 1960, **36**, 147
15 Ward, I. M. and Wilding, M. A. *Polymer* 1977, **18**, 327
16 Levenberg, K. *Q. Appl. Math.* 1944, **2**, 164
17 Cunningham, A., Davies, G. R. and Ward, I. M. *Polymer* 1974, **15**, 743
18 Hutchinson, I. J., Jarvis, D. A., Bower, D. I. and Ward, I. M. *Polymer* 1980, **21**, 41
19 Miller, R. G. J. and Willis, H. A. *J. Polym. Sci.* 1956, **19**, 485
20 Farrow, G. and Ward, I. M. *Polymer* 1960, **1**, 330
21 Schmidt, P. G. *J. Polym. Sci. (A)* 1963, **1**, 1271
22 Abe, Y. and Flory, P. J. *J. Chem. Phys.* 1970, **52**, 2814
23 Robertson, R. E. *J. Chem. Phys.* 1966, **44**, 3950